Proceeding of the IEEE
International Conference on Robotics and Biomimetics
Dali, China, December 2019

Nonlinear identification of IPMC actuators employing RFNN-NARX model and Particle Swarm Optimization

Hongshuai Liu[1], Wenlin Chen[2], Jiaming Chen[3] and Lina Hao[1*], Member, IEEE

***Abstract*—Ionic Polymer Metal Composite (IPMC) is a new smart material that can be used as both sensors and actuators in numerous industrial and medical applications. However, IPMC actuators have many disadvantages, such as hysteresis nonlinearity, which make it difficult to model accurately. In this paper, we presented a precise dynamic nonlinear model with temporal operation for IPMC actuators based on a recurrent fuzzy neural network (RFNN) with interpretability, universal approximation ability and learning ability, a nonlinear auto-regressive with exogenous input (NARX) structure with potential to predict future outputs, Adaptive Weighted Particle Swarm Optimization (AWPSO) algorithm with local and global optimization capability and recurrent least squares (RLS).Firstly, a suitable mathematical model with temporal relations using RFNN-NARX structure was constructed. Then, AWPSO and RLS were employed to identify unknown parameters by using the collected experimental data. Finally, verification results were provided to show the capability of the presented method to effectively and accurately predict the actual displacement of IPMC actuators.**

Keywords—IPMC; identification; fuzzy logic; neural network; particle swarm optimization

I. INTRODUCTION

IPMC is a new type of electroactive polymer (EAP) material with similar electromechanical properties to biological muscles, also known as artificial muscle material [1, 2]. IPMC has recently attracted significant attention in numerous application area, such as microelectromechanical systems (MEMS), medical field, and industrial field [3-8].

Similar to other smart materials, IPMC possesses strong hysteresis nonlinearity [9-11], which make it difficult to model accurately. In order to establish an accurate model of the IPMC actuator, many methods have been proposed in the literature. Brokate et al.[12] and Kanno et al.[13] presented models based on the chemical and physical properties of IPMC. These models are unable to characterize the hysteresis characteristics of IPMC actuators. Since IPMC has strong nonlinear characteristics, it is difficult to establish a precise physical model. According to IPMC response data, Kim et al.[14] presented a fourth-order linear model with no hysteresis characteristics at the Laplace field. In order to capture the strong nonlinear characteristics of IPMC, many nonlinear models were presented in the papers. Kothera et al.[15] proposed a nonlinear model based on Volterra series. Mohsen et al.[16] presented a non-autoregressive nonlinear model used generalized Volterra-based approach. Truong et al.[17] built a nonlinear black box model employed a general multi-layer perceptron neural network. Chi Nama et al.[18, 19]combine fuzzy logic, NARX model and PSO to identified the IPMC. Nadia Naghavi et al.[20, 21]employed ANFIS-NARX paradigm to model the IPMC and later modified the paradigm with hysteresis operator.

The recurrent fuzzy neural network (RFNN) not only combines the function of fuzzy reasoning with the artificial neural network function in learning process modeling, but also uses recursive neurons as internal memory to process internal information [22, 23], which make it interpretable, transparent, and suitable for describing strong hysteresis nonlinearity and creep nonlinearity of the IPMC actuators. In this study, we constructed the RFNN-NARX model to capture the hysteresis nonlinearity for the IPMC actuator, and a learning algorithm combing AWPSO and RLS were used in the RFNN-NARX model, finally, experimental results, model validation and comparison were performed to evaluate the validity and accuracy of the proposed modeling method.

II. RFNN-NARX MODEL

A. RFNN architecture

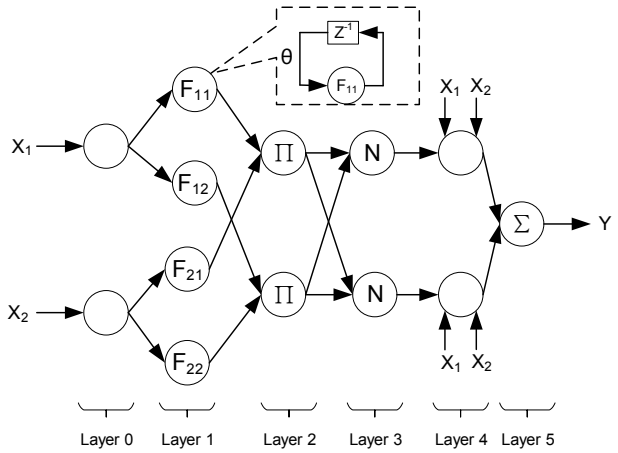

Fig. 1. Structure of RFNN with two inputs and one output.

The RFNN structure used in this paper is the same as Adaptive Neuro-Fuzzy Inference System (ANFIS), except that in this structure, there are recurrent neurons in the fuzzification process as recurrent connections [20, 24, 25]. As illustrated in

[1] School of Mechanical Engineering and Automation, Northeastern University, Shenyang, 110819, China.
[2] School of Resources and Civil Engineering, Northeastern University, Shenyang, 110819, China.
[3] Sino-Dutch Biomedical and Information Engineering School, Northeastern University, Shenyang, 110819, China.
* The corresponding author: Lina Hao (E-mail: haolina@me.neu.edu.cn)

978-1-7281-6321-5/19//$31.00 ©2019 IEEE

Fig. 1, the RFNN structure employed in this paper consists of two input values, one output value, and six layers and temporal operations are established in the artificial neural network by using recurrent connections in the layer 1 of the ANFIS.

This structure is based on some fuzzy inference rules such as the followings:

Rule 1:if x_1 is F_{11} and x_2 is F_{21} then $f_1 = a_1x_1 + b_1x_2$

Rule 2:if x_1 is F_{12} and x_2 is F_{21} then $f_2 = a_2x_1 + b_2x_2$

where a_j and b_j are typical linear consequent parameters; F_{ij} are the fuzzy set; x_1 and x_2 are the network input values, as well.

The layer 0: external input values go through this layer to the next layer with the link weight is unity.

$$O_{ij}^0(t) = u_i^0(t) = x_i(t) \tag{1}$$

where O_{ij}^0 and u_i^0 shows the output and input of the layer 0 for the j th node at time instant t, respectively.

The layer 1: this layer performs the fuzzification process.

Let $\mu_{ij}(t)$ be the Gaussian membership degree of the $n_i(t)$ in the fuzzy set F_{ij}.

$$O_{ij}^1(t) = \mu_{ij}(t) = \exp\left(\frac{-(n_i(t) - m_{ij} - \theta_{ij} * (\mu_{ij}(t-1)))^2}{(\sigma_{ij})^2}\right) \tag{2}$$

where n_i and O_{ij}^1, are the node input value and output value of the layer 1 at time instant t, respectively; m_{ij} and σ_{ij} are the center and the width of the Gaussian membership function; A very important nature at this layer is that θ_{ij} reflects the feed weight in the feedback loop. At the layer 1, m_{ij}, θ_{ij} and σ_{ij} are three adjustable parameters. Obviously, the input to this layer contains memory terms $\mu_{ij}(t-1)$, which stores the previous information of the network. Compared with ANFIS, RFNN has a memory effect by adding this recurrent structure. The RFNN has time-varying fuzzy kernels through such recurrent neurons, rather than being fixed. As is shown in fig. 2 [24], the nonlinear mapping using the time-varying kernel fuzzy sets between input and output values is no longer single, static, but time-varying, and dynamic, according to the input signal values of the external world. This mechanism allows the RFNN to have the ability to handle unfixed inputs and outputs through internal time operations, which makes the RFNN clearly distinguishable from ANFIS with only feedforward connections.

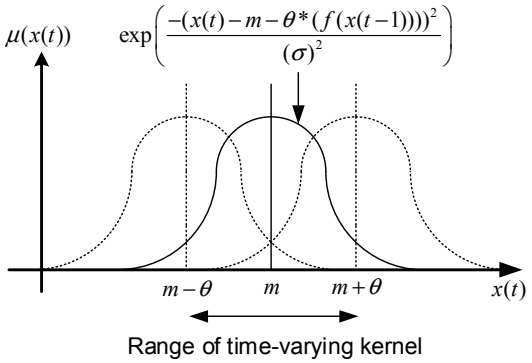

Fig. 2. Fuzzy set with time-varying kernel.

The layer 2: the firing strength of each rule is calculated by the product of all the input values at this layer.

$$O_i^2 = \overline{\mu}_i(t) = \prod_{j=1}^{n} n_{ij}(t) = \prod_{j=1}^{n} \mu_{ij}(t) \tag{3}$$

The layer 3: the normalization firing strengths is performed at this layer.

$$O_i^3 = w_i(t) = \frac{\overline{\mu}_i(t)}{\sum_{i=1}^{L} \overline{\mu}_i(t)} \tag{4}$$

The layer 4: each output value at this layer has a mathematic expression as follows:

$$O_i^4 = w_i\left(a_ix_1 + b_ix_2\right) \quad i = 1, 2, \cdots \tag{5}$$

The layer 5: the final output value is generated by calculating the summation of all input values.

$$O_i^5 = \sum_{i=1}^{n} w_i\left(a_ix_1 + b_ix_2\right) \quad i = 1, 2, \cdots \tag{6}$$

B. NARX model

The NARX model can represent various nonlinear systems by nonlinearly mapping past input values, output values, and noise term values with future output values, and the NARX model formula as follows:[26, 27]

$$\begin{aligned} y(t) = f\big(&y(t-1), \ldots, y\left(t-n_y\right), \\ &u(t-d-1), \ldots, u\left(t-d-n_u\right)\big) + \xi(t) \end{aligned} \tag{7}$$

where d denotes the known system delay time. $y(t)$, $y(t-1)$, $u(t-1)$ and $\xi(t)$ are future output values, past input values, output values and noise values, respectively.

C. RFNN-NARX model

In the formula (7) of NARX model, the nonlinear mapping function f is unknown, and RFNN is a universal approximator combining fuzzy reasoning and artificial neural network, and with internal memory, so NARX and RFNN are combined to form RFNN-NARX model, where the role of the RFNN is to approximate the nonlinear mapping function f.

RFNN-NARX model has both the benefits of artificial neural networks and fuzzy inference, and with memory operations, which can map out future output values depending on the past input values and output values of the nonlinear plant, which makes it suitable for capturing the strong hysteresis and nonlinear characteristics of the IPMC.

When using RFNN to approximate f, the model formula (7) can be rewritten as:

R_j : IF $x_1(t)$ is F_{1j}, ..., $x_i(t)$ is F_{ij}, ..., and $x_n(t)$ is F_{nj}

Then

$$y_j(t) = a_j\left(z^{-1}\right)y(t-1) + b_j\left(z^{-1}\right)u(t-d) + \xi(t) \quad (8)$$

$$a_j\left(z^{-1}\right) = a_{j,1} + a_{j,2}z^{-1} + \cdots + a_{j,\ n_y}z^{-(n_y-1)}$$

$$b_j\left(z^{-1}\right) = b_{j,0} + b_{j,1}z^{-1} + b_{j,2}z^{-2} + \cdots + b_{j,n_u}z^{-n_u}$$

where $x_i(t)$, and $y_j(t)$ are input at layer 0 and output at layer 4 of the RFNN model at time t, respectively. F_{ij} is the fuzzy set corresponding to $x_i(t)$ in the j th fuzzy implication, and $n = n_y + n_u$.

In the case where the number of fuzzy rules is L, the complete RFNN-NARX model, which is the output of layer 5 in the RFNN structure, can be written as follows:[23, 28]

$$y(t) = \sum_{j=1}^{L} w_j(t)\left[a_j\left(z^{-1}\right)y(t-1) + b_j\left(z^{-1}\right)u(t-1)\right] + \xi(t) \quad (9)$$

where the calculation method of $w_j(t)$ is shown in (2), (3), and (4).

D. Training algorithm of RFNN-NARX model

The antecedent parameters (m_{ij}, θ_{ij}, σ_{ij}) and consequent parameters (a_i, b_i) are unknown in the RFNN-NARX model and need to be identified by the training algorithm.

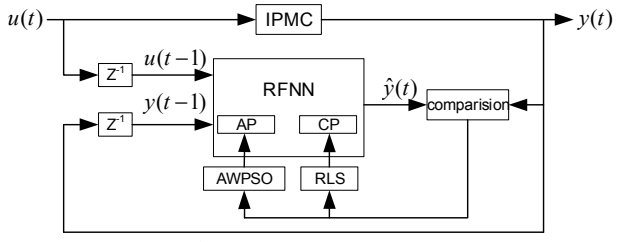

Note. AP= antecedent parameters, CP= consequent parameters.

Fig. 3. RFNN-NARX model with PSO and RLS identification scheme

There are many approaches to identify unknown parameters, such as genetic algorithm (GA), particle swarm optimization (PSO), backpropagation learning algorithm (BP), gradient descent (GD), least squares (LS), and recurrent least squares (RLS). PSO is an advanced swarm intelligence algorithm with good local and global exploration ability. The RLS algorithm converges quickly and is easy to understand. Therefore, as is shown in fig. 3, AWPSO was used to identify the antecedent parameters and RLS was employed to identify the consequent parameters.

III. Experimental Equipment and Data

The physical experimental system, as shown in fig. 4, mainly consists of an IPMC strip ($20\times7\times0.3\text{mm}^3$), an OADM2016441/S14F laser displacement sensor (1 mm V−1), a desktop PC with MATLAB/Simulink installed, a homemade power amplifier, and an NI DAQ card (PCI 6221 16-bit A/D D/A converter). The experiments were performed on a shock absorber table. In the experiment, the signal duration used was 100s and the sampling interval was 0.01s, so 10000 data points were obtained for each experiment.

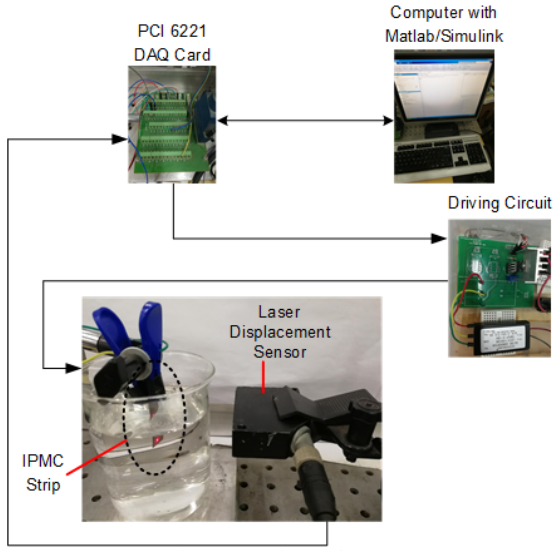

Fig. 4. Experimental setup.

The excitation signals are chosen as chirp signal, single-tone sinusoidal signal and dual-tone sinusoidal signal defined by

$$\text{chirp}(t) = A\sin\left(\omega_1 t + \frac{(\omega_2-\omega_1)}{2M}t^2\right) \quad (10)$$

$$\text{single\_sin}(t) = A\sin(2\pi\omega t) \quad (11)$$

$$\text{dual\_sin}(t) = A_1\sin\left(2\pi\omega_1 t\right) + A_2\sin\left(2\pi\omega_2 t\right) \quad (12)$$

where A represents the amplitude and ω stands for the frequency, respectively.

TABLE I. Characteristics of the Excitation Signal

Signal	Frequency (Hz)	Amplitude (V)
Chirp signal	0-0.3	3
Single-tone sinusoidal signal	0.1	3
Dual-tone sinusoidal	0.1 and 0.05	2 and 1

The chirp signal is an excitation signal with wide frequency range and is often used in model identification to obtain the response characteristics of the IPMC at all operating frequencies. Therefore, we use the IPMC displacement response data set generated by the chirp excitation signal as the training data set. Experimental data obtained under the other

two signals was used as a test data set. Table I describes the specific parameters of the excitation voltage signal.

IV. Experimental Results

In this part, we want to experimentally verify the RFNN-NARX model proposed in the above section, firstly, we need to determine the order of the RFNN-NARX model. In theory, the higher the model order, the more accurate the model, but it will also bring more computational complexity, so we choose the one-order model, i.e., $n_y = 1, n_u = 1, d = 1$. then the model formula (7) can be rewritten as:

$$y(t) = f\left(y(t-1), u(t-1)\right) \tag{13}$$

Each input variable was divided into 5 fuzzy subsets, so there were 25 fuzzy rules for the 2 input variables.

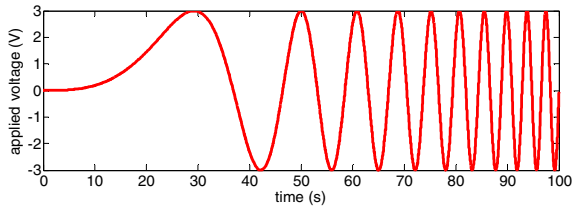

Fig. 5 (a). Applied voltage signal curve.

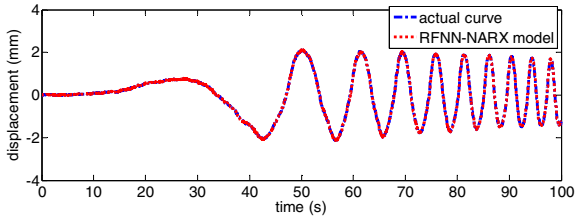

Fig. 5 (b). RFNN-NARX model and actual displacement curve of IPMC.

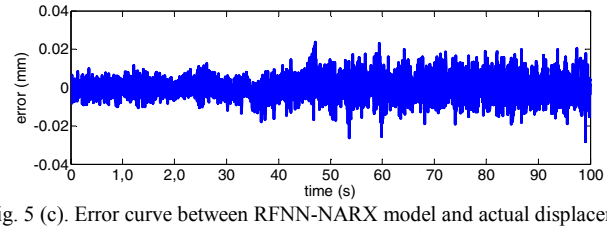

Fig. 5 (c). Error curve between RFNN-NARX model and actual displacement.

Fig. 5. Training result with input chirp signal.

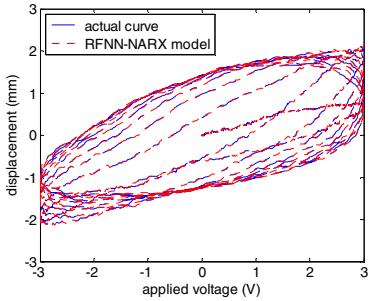

Fig. 6. IPMC displacement versus chirp input signal.

In the above parameter selection, it proved to be reasonable in computer simulation. Then chirp input–output signal data was employed as training data set, and the other two signals data were employed for model validation. The estimation results were shown in fig. 5 to 10, respectively. It can be seen from the training and test results graph that the RFNN-NARX model proposed in this paper has high estimation accuracy for the hysteretic nonlinear displacement response of the IPMC.

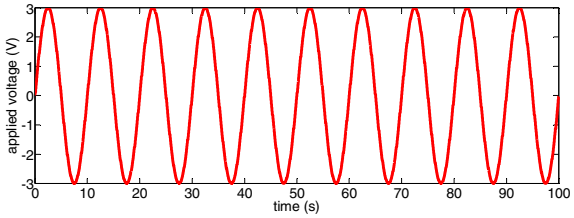

Fig. 7 (a). Applied voltage signal curve.

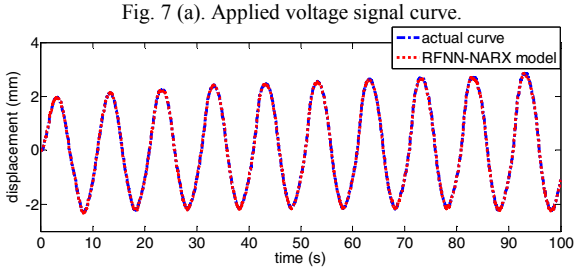

Fig. 7 (b). RFNN-NARX model and actual displacement curve of IPMC.

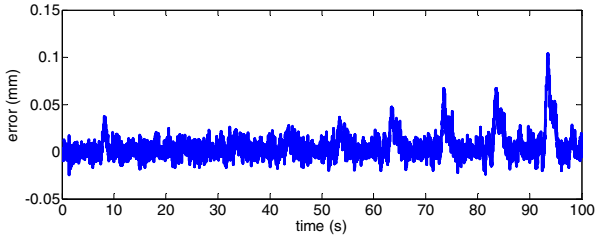

Fig. 7 (c). Error curve between RFNN-NARX model and actual displacement.

Fig. 7. Validating result with input single-tone sinusoidal signal.

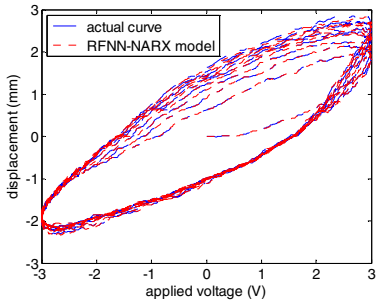

Fig. 8. IPMC displacement versus single-tone sinusoida input signal.

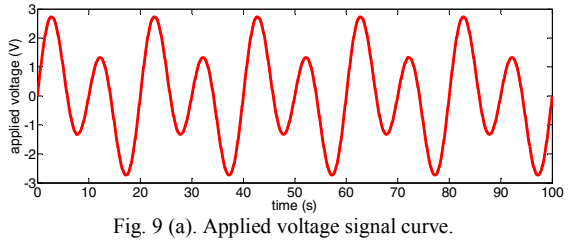

Fig. 9 (a). Applied voltage signal curve.

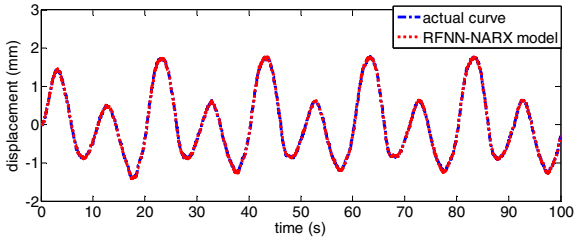

Fig. 9 (b). RFNN-NARX model and actual displacement curve of IPMC.

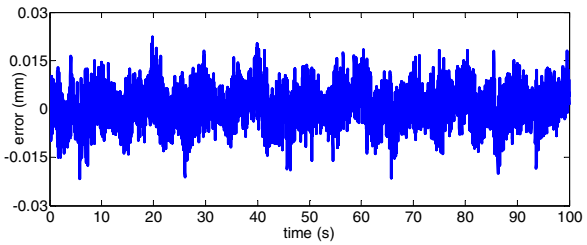

Fig. 9 (c). Error curve between RFNN-NARX model and actual displacement.
Fig. 9. Validating result with input dual-tone sinusoidal signal.

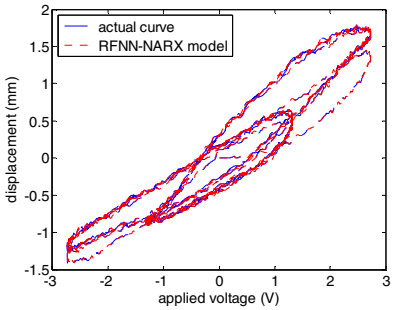

Fig. 10. IPMC displacement versus dual-tone sinusoidal input signal.

TABLE II. THE COMPARISON OF MSE BETWEEN TWO MODELS

MSE	Input signal	RFNN-NARX model	ANFIS-NARX model
Train	Chirp	2.8555e-5	6.0967e-5
Test	Single-tone sine	2.0468e-4	2.2055e-4
Test	Dual-tone sine	3.1112e-5	6.5321e-5
	Mean	8.8114e-5	11.561e-5

In order to do the comparison, in the RFNN-NARX model and the ANFIS-NARX model antecedent parameter identification process, the PSO algorithm is set to the same initialization parameters (the initial particle is 30 and the stopping criterion is to iteration 100 times). The mean square error (MSE) of the two models was compared using the Chirp signal data as training samples, and the other two signals data were used as test samples. The comparison results of MSE between two models were shown in table II. In the training and test data sets, the MSE value of the RFNN-NARX model is significantly smaller than the MSE of the ANFIS-NARX model, which indicates RFNN-NARX model with more universality and better generalization ability to better capture IPMC bending behavior with higher accuracy.

V. CONCLUSIONS AND FUTURE WORK

In this paper, we proposed an accurate dynamic RFNN-NARX model for IPMC that combines neural networks with internal feedback and fuzzy logic, and used AWPSO and RLS to identify unknown parameters. It is verified by experiments that the RFNN-NARX model with universality and generalization ability can well capture the strong hysteresis nonlinear characteristics of IPMC, and has a high estimation accuracy for the actual output displacement of IPMC.

In the future work, we will design the controller based on the RFNN-NARX model to complete the precise displacement control of IPMC in practical application tasks.

ACKNOWLEDGMENT

The authors would like to thank Jinhai Gao for providing guidance on the experiments of IPMC. This work is supported by National Nature Science Foundation under Grant 61573093.

REFERENCES

[1] M. Shahinpoor and K. J. Kim, "Ionic polymer-metal composites: I. Fundamentals," (in English), *Smart Materials & Structures,* vol. 10, no. 4, pp. 819-833, Aug 2001.
[2] Y. Bar-Cohen and Y. Bar-Cohen, *Electroactive polymer (EAP) actuators as artificial muscles: reality, potential, and challenges*. SPIE press Bellingham, WA, 2004.
[3] M. Shahinpoor and K. J. Kim, "Ionic polymer–metal composites: IV. Industrial and medical applications," *Smart materials and structures,* vol. 14, no. 1, p. 197, 2004.
[4] H. R. Cheong, C. Y. Teo, P. L. Leow, K. C. Lai, and P. S. Chee, "Wireless-powered electroactive soft microgripper," (in English), *Smart Materials And Structures,* vol. 27, no. 5, May 2018.
[5] H. R. Cheong, N. T. Nguyen, M. K. Khaw, B. Y. Teoh, and P. S. Chee, "Wirelessly activated device with an integrated ionic polymer metal composite (IPMC) cantilever valve for targeted drug delivery," (in English), *Lab on a Chip,* vol. 18, no. 20, pp. 3207-3215, Oct 21 2018.
[6] K. C. Aw and A. J. McDaid, "Bio-applications of ionic polymer metal composite transducers," (in English), *Smart Materials And Structures,* vol. 23, no. 7, Jul 2014.
[7] P. Brunetto, L. Fortuna, P. Giannone, S. Graziani, and F. Pagano, "A Resonant Vibrating Tactile Probe for Biomedical Applications Based on IPMC," (in English), *Ieee Transactions on Instrumentation And Measurement,* vol. 59, no. 5, pp. 1453-1462, May 2010.
[8] Y. Chen, L. N. Hao, H. Yang, and J. H. Gao, "Kriging modeling and SPSA adjusting PID with KPWF compensator control of IPMC gripper for mm-sized objects," (in English), *Review Of Scientific Instruments,* vol. 88, no. 12, Dec 2017.
[9] X. B. Tan and J. S. Baras, "Adaptive identification and control of hysteresis in smart materials," (in English), *Ieee Transactions on Automatic Control,* vol. 50, no. 6, pp. 827-839, Jun 2005.
[10] L. Hao and Z. Li, "Modeling and adaptive inverse control of hysteresis and creep in ionic polymer–metal composite actuators," *Smart Materials and Structures,* vol. 19, no. 2, p. 025014, 2010.
[11] K. K. Ahn, D. Q. Truong, D. N. C. Nam, J. I. Yoon, and S. Yokota, "Position control of ionic polymer metal composite actuator using quantitative feedback theory," *Sensors and Actuators A: Physical,* vol. 159, no. 2, pp. 204-212, 2010.
[12] M. Brokate and J. Sprekels, *Hysteresis and phase transitions*. Springer Science & Business Media, 2012.
[13] R. Kanno, S. Tadokoro, T. Takamori, M. Hattori, and K. Oguro, "Linear approximate dynamic model of ICPF (ionic conducting polymer gel film) actuator," in *Proceedings of IEEE International Conference on Robotics and Automation*, 1996, vol. 1, pp. 219-225: IEEE.
[14] N. D. Bhat and W.-j. Kim, "Precision position control of ionic polymer metal composite," in *Proceedings of the 2004 American control conference*, 2004, vol. 1, pp. 740-745: IEEE.
[15] C. S. Kothera and D. J. Leo, "Identification of the nonlinear response of ionic polymer actuators using the Volterra series," *Journal of Vibration and Control,* vol. 11, no. 4, pp. 519-541, 2005.
[16] M. Annabestani, N. Naghavi, and M. M. Nejad, "Nonautoregressive nonlinear identification of IPMC in large deformation situations using generalized Volterra-based approach," *IEEE Transactions on Instrumentation and Measurement,* vol. 65, no. 12, pp. 2866-2872, 2016.
[17] D. Quang Truong and K. Kwan Ahn, "Design and verification of a non-linear black-box model for ionic polymer metal composite actuators," *Journal of intelligent material systems and structures,* vol. 22, no. 3, pp. 253-269, 2011.
[18] N. D. N. Chi, T. D. Quang, J. I. Yoon, and K. K. Ahn, "Identification of ionic polymer metal composite actuator employing fuzzy NARX model and Particle Swam Optimization," in *2011 11th International Conference on Control, Automation and Systems*, 2011, pp. 1857-1861: IEEE.
[19] D. N. C. Nam and K. K. Ahn, "Identification of an ionic polymer metal composite actuator employing Preisach type fuzzy NARX model and particle swarm optimization," *Sensors and Actuators A: Physical,* vol. 183, pp. 105-114, 2012.

[20] M. Annabestani and N. Naghavi, "Nonlinear identification of IPMC actuators based on ANFIS–NARX paradigm," *Sensors and Actuators A: Physical,* vol. 209, pp. 140-148, 2014.
[21] H. Zamyad, N. Naghavi, and H. Barmaki, "A combined fuzzy logic and artificial neural network approach for non-linear identification of IPMC actuators with hysteresis modification," (in English), *Expert Systems,* vol. 35, no. 4, Aug 2018.
[22] C. F. Juang and C. T. Lin, "A recurrent self-organizing neural fuzzy inference network," (in English), *Ieee Transactions on Neural Networks,* vol. 10, no. 4, pp. 828-845, Jul 1999.
[23] C. H. Lu and C. C. Tsai, "Generalized predictive control using recurrent fuzzy neural networks for industrial processes," (in English), *Journal Of Process Control,* vol. 17, no. 1, pp. 83-92, Jan 2007.
[24] C. Li and K. H. Cheng, "Recurrent neuro-fuzzy hybrid-learning approach to accurate system modeling," (in English), *Fuzzy Sets And Systems,* vol. 158, no. 2, pp. 194-212, Jan 16 2007.
[25] M. A. Khanesar, M. A. Shoorehdeli, and M. Teshnehlab, "Hybrid training of recurrent fuzzy neural network model," (in English), *2007 Ieee International Conference on Mechatronics And Automation, Vols I-V, Conference Proceedings,* pp. 2598-2603, 2007.
[26] T. A. Johansen and B. FOSS, "Constructing NARMAX models using ARMAX models," *International Journal of Control,* vol. 58, no. 5, pp. 1125-1153, 1993.
[27] S. Chen and S. A. Billings, "Representations of non-linear systems: the NARMAX model," *International Journal of Control,* vol. 49, no. 3, pp. 1013-1032, 1989.
[28] C. C. Hsiao, S. F. Su, T. T. Lee, and C. C. Chuang, "Hybrid compensation control for affine TSK fuzzy control systems," (in English), *Ieee Transactions on Systems Man And Cybernetics Part B-Cybernetics,* vol. 34, no. 4, pp. 1865-1873, Aug 2004.